

Abstract

LEWANDOWSKI, DAVID JOHN **Experimental and Modeled Effects of Camshaft Manufacturing Errors on the Dynamics of High Speed Valve Trains.** (Under the direction of Dr. Joseph W. David)

The idea of harnessing combustion to perform mechanical work is by no means a new one. The internal combustion engine, as we know it today, has its origins in the last century, however the idea for controlling combustion to perform mechanical work dates back to the Renaissance. Even with the advent of alternative sources of power for commerce and personal applications, the internal combustion engine represents a large portion of the power generation available in this country.

There are numerous types of internal combustion engines, each with a variety of subsystems. While all of these types and corresponding subsystems are equally important, this investigation is focused on the valve train dynamics of a pushrod type internal combustion engine. Operating this type of engine at too high of an engine speed usually causes dynamic malfunctions such as spring surge, lifter/cam pair separation, valve bounce, etc. in the valve train. Although the interaction of each of the valve train components contributes to the limit speed, the shape of the cam plays a critical role. Therefore, this investigation will look at how small changes in the cam profile due to manufacturing errors change the dynamics of a valve train in a pushrod type engine.

Automotive cams can be manufactured as copied or original parts. Copied parts are typically produced on a rocker type cam grinder and the original parts are produced on

a computer numerical control grinder. Therefore, various errors associated with these manufacturing techniques are studied herein.

Installing cams with profile errors in an engine may result in the dynamic malfunction of its valve train. In order to study the effect of these profile errors, some of the error cam profiles that were predicted for the rocker grinder were manufactured and tested in an actual valve train. In addition, the effects of error cam profiles were investigated by using an existing valve train simulation model. It was found by both experimentation and simulation that camshaft errors on the order of typical shop tolerances had little impact on the dynamics of high speed valve trains.

Experimental and Modeled Effects of Camshaft Manufacturing Errors on the Dynamics of High Speed Valve Trains

by

David J. Lewandowski

A thesis submitted to the Graduate Faculty of
North Carolina State University
in partial fulfillment of the
requirements for the Degree of

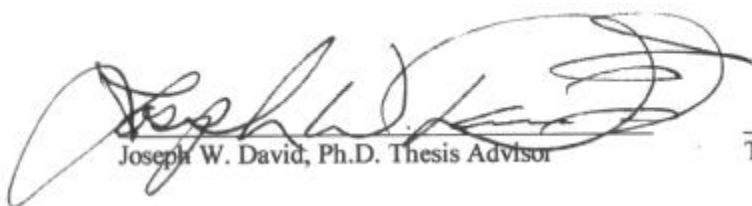
Doctor of Philosophy

Department of Mechanical and Aerospace Engineering

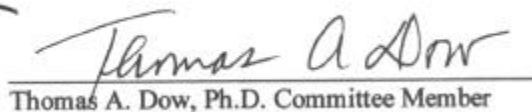
Raleigh

1998

Approved By:



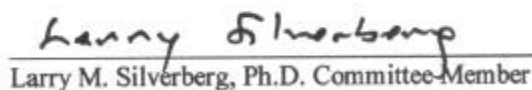
Joseph W. David, Ph.D. Thesis Advisor



Thomas A. Dow, Ph.D. Committee Member



James F. Selgrade, Ph.D. Committee Member



Larry M. Silverberg, Ph.D. Committee Member

for my wife, Eileen; and son, David Jr.

Biography

The author was born in Yonkers, New York on October 18, 1965. He attended Saunders Trade and Technical High School in Yonkers to study Mechanical Technology and graduated with honors June 1983. During his senior year in high school, he started work at Synchro-Motion Corporation as a machinist.

While working at Synchro-Motion, the author attended Manhattan College in Riverdale, New York for his bachelors degree and graduated with honors in May 1987. Upon graduation, he was employed by Malcolm Pirnie, Incorporated. At Malcolm Pirnie, the author worked on a variety of solid waste and wastewater projects. He returned to night school in January 1991 and graduated with a Masters Degree in May 1993 from Manhattan College. More importantly during this time, the author was married on Halloween 1992.

The author enrolled in graduate school in August 1993 at North Carolina State University in Raleigh. In August 1997, the author and his wife had their first child, David, Jr.

Acknowledgments

I would like to thank my good friend and mentor, Dr. Joseph W. David, for giving me this opportunity to perform this research. Without him I would not have learned nearly as much about research as I do now. I would also like to thank Dr. Thomas Dow, Dr. Larry Silverberg and Dr. James Selgrade for serving on my graduate committee.

I would like to thank Brian Mitchell, Clark Park, Erik 'E. Z. Ike' Lowndes, Gerrit 'G-Money' Gast, Mark 'Stroh-Dogg' Strohmeyer, 'Crazy' Dave Robbins, Chien Ying 'MIT' Cheng, Mason 'Dixon' Kenyon, Mark 'Satan' Etheridge and Jarn-'holi'-o Kilian, for not only their help during this research but for providing a kick in the butt or a good laugh as needed.

I would also like to thank Joe dos Santos, Frank Krasovic and Tony Pacaro. Finer friends no man can ask for.

A big thanks goes to Jesel, Inc., especially Walter Donovan and Dan Jesel, for their willingness to supply parts and technical expertise for this research. In addition, this research would have been nearly impossible without large quantities of Diet Coke, Judas Priest and the Beastie Boys.

Finally, I more than thank all of my family, especially my wife, Eileen, and son, David Jr. who have supported me throughout this research (financially and otherwise) and have patiently endured way too much in my quest for this degree.

Table of Contents

List of Figures	viii
List of Tables	xii
List of Symbols	xiii

1 Introduction

1.1	Early Engine Development	1
1.2	Comparison of Installed Power Consumption	3
1.3	Brief Description of Valve Train Motion	4
1.4	Valve Train – Then and Now	7
1.5	Discussion of Cam Motion, Profile Errors and Tolerances	8
1.6	Objective	11
1.7	Valve Train Dynamics	13
1.8	Cam Manufacturing Options	16
1.9	Original Plate Cam Manufacture	17
1.10	Copied Plate Cam Manufacture	28
1.11	Overview of the Thesis	30

2 Development of a Kinematic Model for the Rocker Type Cam Grinder

2.1	Selection of the Rocker Grinder Model	33
2.2	Kinematic Model Overview	33
2.3	Cam Motion Analysis	34
2.4	Fourier Series as a Motion Analysis Tool	35

2.5	Design of Cam Profiles	37
2.6	Constraint Conditions	39
2.7	Description of the Rocker Grinder Operation	41
2.8	Analysis Outline for the Grinder Model	42
2.9	Theoretical Cam Grinder Model	43
2.10	Kinematic Model of the Actual Grinding Mechanism	45
2.11	Actual Cam Profile Due to Grinding Wheel Variation in Rocker Mechanism	47
2.12	Actual Cam Profile Generation Due to Link Length Variation	49
2.13	Determination of a Lift Curve for Flat Follower Cam for a Given Cam Profile	50
2.14	Determination of Lift Curve for Roller Follower Cam	51
2.15	Determination of Equidistant Lift, Velocity and Acceleration Curves	52
3	Results of the Rocker Type Grinder Simulation	
3.1	Objective	53
3.2	Theoretical Link Dimensions	54
3.3	Variation in Grinding Wheel Diameter	58
3.4	Variation in Rocker Length	62
3.5	Variation in Vertical Grinding Wheel Position	67
3.6	Discussion of Results	71
4	Experimental Studies of Valve Train Dynamics	
4.1	Objective of Experiments	73

4.2	Experimental Apparatus	73
4.3	Modular Camshaft Construction	76
4.4	Baseline Experiments Concerning Valve Train Behavior	79
4.5	Comparison of Test Results for an Actual Automotive Camshaft and the Modular Cam	84
4.6	Experimental Determination of the Effects of Grinding Wheel Size Error on Valve Train Dynamics	86
5	Simulation of the Effects of Predicted and Actual Cam Errors on Valve Train Dynamics	
5.1	Objective of the Simulations	88
5.2	Valve Train Model	88
5.3	Results of Valve Train Simulations for Cam Profiles with Grinding Wheel Diameter Errors	92
5.4	Results of Valve Train Simulations for Cam Profiles with Rocker Length Variation and Vertical Wheel Position Errors	96
5.5	Overview of the CNC Error Investigation	99
5.6	Actual CNC Error Data	100
5.7	Simulations Using the CNC Grinder Error	101
6	Results and Conclusions	
6.1	Conclusions	104
6.2	Implications of the Study	104
6.3	Recommendations	106
	References	108

List of Figures

1.1	Comparison of estimated available power for power plants and automobiles in the Raleigh, NC area served by CP&L	4
1.2	Various valve train configurations	5
1.3	Valve train schematic	6
1.4	Short range experimental valve bounce comparison	15
1.5	Amplitude of valve bounce for entire engine operating range	15
1.6	Typical multi-lobe internal combustion engine camshaft	16
1.7	Rocker type cam grinder schematic	29
1.8	Flowchart of cam error research	31
2.1	Cam lift measuring equipment	35
2.2	Schematic of a cam with a translating flat follower	38
2.3	Schematic of a cam with a translating roller follower	39
2.4	Schematic of general cam/roller follower pair contact conditions	40
2.5	Schematic of the theoretical cam grinder rocker mechanism	42
2.6	Schematic of the actual grinding loop	46
3.1	Schematic of the theoretical cam grinder rocker mechanism	54
3.2	Camshaft nomenclature for cam base circle sizing	56
3.3	Theoretical cam lift curve	56
3.4	Theoretical cam velocity curve	57
3.5	Theoretical cam acceleration curve	57

3.6	Normalized flat follower cam lift error due to grinding wheel diameter change	59
3.7	Normalized flat follower cam velocity error due to grinding wheel diameter change	60
3.8	Normalized flat follower acceleration error due to grinding wheel diameter change	60
3.9	Normalized roller follower cam lift error due to grinding wheel diameter change	61
3.10	Normalized roller follower cam velocity error due to grinding wheel diameter change	61
3.11	Normalized roller follower cam acceleration error due to grinding wheel diameter change	62
3.12	Normalized flat follower cam lift error due to rocker length change	64
3.13	Normalized flat follower cam velocity error due to rocker length change	64
3.14	Normalized flat follower cam acceleration error due to rocker length change	65
3.15	Normalized roller follower cam lift error due to rocker length change	65
3.16	Normalized roller follower cam velocity error due to rocker length change	66
3.17	Normalized roller follower cam acceleration error due to rocker length change	66
3.18	Normalized flat follower cam lift error due to vertical wheel position change	68
3.19	Normalized flat follower cam velocity error due to vertical wheel position change	69
3.20	Normalized flat follower cam acceleration error due to vertical wheel position change	69
3.21	Normalized roller follower cam lift error due to vertical wheel position change	70

3.22	Normalized roller follower cam velocity error due to vertical wheel position change	70
3.23	Normalized roller follower cam acceleration error due to vertical wheel position change	71
4.1	Schematic of the test rig used to experimentally investigate valve train dynamics	74
4.2	Photograph of actual test equipment	74
4.3	Exploded view of modular cam components	77
4.4	Assembled view of modular cam components	77
4.5	Comparison of flat follower lobes manufactured by edm to show wear due to improper cam/follower match	79
4.6	Valve bounce comparison for two cylinders during the same test using a full valve train	80
4.7	Difference in cam lift for two cylinders on same camshaft	81
4.8	Baseline test data for comp cams 938 type springs	83
4.9	Baseline test data for k motion 1600 type springs	83
4.10	Comparison of actual camshaft and modular cam results for comp cams 938 spring type	85
4.11	Comparison of actual camshaft and modular cam results for k-motion 1600 spring type	85
4.12	Error cam test data for the comp cams 938 type spring	86
4.13	Error cam test data for the k motion 1600 type spring	87
5.1	Lumped mass and fea model of valve train	90
5.2	Simulated and experimental data for the cam generated using a 0.406 meter (16 inch) grinding wheel using the comp cams 938 spring	93

5.3	Simulated and experimental data for the cam generated using a 0.305 meter (12 inch) grinding wheel and the comp cams 938 spring	94
5.4	Simulated and experimental data for the cam generated using a 0.203 meter (8 inch) grinding wheel and the comp cams 938 spring	94
5.5	Simulated and experimental data for the cam generated using a 0.406 meter (16 inch) grinding wheel and the k motion 1600 spring	95
5.6	Simulated and experimental data for the cam generated using a 0.305 meter (12 inch) grinding wheel and the k motion 1600 spring	95
5.7	Simulated and experimental data for the cam generated using a 0.206 meter (8 inch) grinding wheel and the k motion 1600 spring	96
5.8	Simulated data for the cam generated using various rocker link lengths and the comp cams 938 spring	97
5.9	Simulated data for the cam generated using various vertical grinding wheel vertical positions and the comp cams 938 spring	98
5.10	Simulated data for the cam generated using various rocker link lengths and the k motion 1600 spring	98
5.11	Simulated data for the cam generated using various vertical grinding wheel vertical positions and the k motion 1600 spring	99
5.12	Extreme lift curve error from a prototype cam produced on a cnc grinder	100
5.13	Valve train simulation using the four original cnc error plots and the comp cams 938 spring	102
5.14	Valve train simulation using the four doubled cnc error plots and the comp cams 938 spring	102
5.15	Valve train simulation using the four original cnc error plots and the k motion 1600 spring	103
5.16	Valve train simulation using the four doubled cnc error plots and the k motion 1600 spring	103

List of Tables

3.1	Maximum and rms errors for flat follower cam due to wheel size change	59
3.2	Maximum and rms errors for roller follower cam due to wheel size change	59
3.3	Maximum and rms errors for flat follower cam due to rocker length change	63
3.4	Maximum and rms errors for roller follower cam due to rocker length change	63
3.5	Maximum and rms errors for flat follower cam due to vertical grinding wheel position change	68
3.6	Maximum and rms errors for roller follower cam due to vertical grinding wheel position change	68
4.1	Nominal parameters of the two spring types used in this investigation	82

List of Symbols

Chapter 2

$a_0 \dots a_n$	cosine coefficients for the Fourier Series
b_n	sine coefficients for the Fourier Series
\hat{c}	cam fixed coordinate system
\bar{d}	general roller follower radius vector
f_{d_i}	discrete lift data used to calculate Fourier Series
f_f	Fourier Series
i	number of discrete data points used in the Fourier Series
Δl	change in rocker length for the rocker cam grinder
l_a	actual rocker length for the rocker cam grinder
l_t	theoretical rocker length for the grinder mechanism
$lift$	desired lift of the cam follower
\hat{m}	outward normal of cam surface
n	summation variable for the Fourier Series
N	number of data points used in the Fourier Series
\hat{n}	ground fixed coordinate system
$ncoeff$	number of coefficients used in the Fourier Series
P	contact point between cam and roller follower
q	center of generic roller follower
r_b	base circle radius
r_f	roller follower radius
\bar{r}_f	vector actual grinding wheel radius
\bar{R}_f	distance vector between center of ground cam and the grinding wheel for the actual rocker cam grinding system
R_n	general loop vectors for the generic roller follower system
\bar{R}_p	vector of point of contact of cam and grinding wheel with respect to the cam center
r_{wa}	actual grinding wheel radius (scalar)
r_{wt}	theoretical grinding wheel radius
S_n	some more general loop vectors for the generic roller follower system
\hat{t}	tangent of cam surface
\tilde{X}	theoretical cam coordinate in the \hat{c}_1 direction
\tilde{X}_a	actual cam coordinate in the \hat{c}_1 direction
x_{ba}	actual \hat{n}_1 distance from rocker pivot to center of grinding wheel

x_{bt}	theoretical \hat{n}_1 distance from rocker pivot to center of grinding wheel
X_c	distance between center of ground cam and the grinding wheel for the actual rocker cam grinding system in the \hat{n}_1 direction
y	overall position of the follower including the base circle radius and follower radius (as required)
y'	overall cam follower velocity
\tilde{Y}	theoretical cam coordinate in the \hat{c}_2 direction
y_{ba}	actual \hat{n}_2 distance from rocker pivot to center of grinding wheel
y_{bt}	theoretical \hat{n}_2 distance from rocker pivot to center of grinding wheel
\tilde{Y}_a	actual cam coordinate in the \hat{c}_2 direction
Y_c	distance between center of ground cam and the grinding wheel for the actual rocker cam grinding system in the \hat{n}_2 direction
Δy	change in vertical grinding wheel position for the rocker cam grinder
a	cam angle
b	cam angle for cam in the rocker grinder
d	variation (due to uncertainty)
g	contact angle from center of grinding wheel to the point of contact with the cam for the rocker mechanism (with respect to ground)
y	rotation angle used to line up actual cam normal with the follower
Φ	angle of rocker link with respect to ground
r	general roller follower radius (scalar)

Chapter 5

a	length from rocker pivot center to contact with pushrod
b	length from rocker pivot center to contact with valve stem
c_1	damping coefficient between cam surface and lifter contact
c_2	damping coefficient between lifter and rocker contact
c_2	damping coefficient between rocker and valve stem contact
$d(t)$	kinematic cam displacement
$\dot{d}(t)$	kinematic cam velocity
E_v	modulus of elasticity of the valve head
$\{F\}$	external forces on the springs (valve spring reaction force and Coulomb damping)
f_{fric}	friction force on valve stem
f_{spring}	spring force on valve stem
h	average valve head stiffness
i	counting variable
$[K]$	stiffness matrix for the valve spring equations of motion
$[\tilde{K}]$	stiffness matrix for the combined model

k_1	contact stiffness between cam surface and lifter
k_2	contact stiffness between equivalent lifter/pushrod and rocker
k_3	contact stiffness between rocker and valve stem
k_4	valve seat stiffness
k_v	valve head equivalent stiffness
$[M]$	lumped mass matrix for the valve springs
$[\tilde{M}]$	lumped mass matrix for the entire model
m_1	equivalent mass of lifter and half of pushrod
m_3	equivalent mass of valve stem and valve head (depending on contact)
n	cam cycle number
n_{fric}	rocker arm friction torque
r_v	valve head radius
v_{lash}	lash between valve and rocker when engine is warm
y_1	displacement of mass m_1
y_3	displacement of valve head
y_4	displacement of valve seat surface
$[\bar{z}]$	displacement of spring nodes in FEA model
J_2	rotation of rocker arm about center pivot
V	valve spring damping coefficient